Potential of functional MREIT to Detect Neural Activity Related Conductivity Changes: Numerical Simulation Studies

Hyung Joong Kim[1], Zijun Meng[1], Saurav ZK Sajib[1], Woo Chul Jeong[1], Young Tae Kim[1], Rosalind J Sadleir[2], and Eung Je Woo[1]
[1]*Biomedical Engineering, Kyung Hee University, Yongin, Gyeonggi, Korea, Republic of,* [2]*University of Florida, Gainesville, Florida, United States*

Purpose

In this study, we are interested in determining the feasibility of applying functional MREIT to image *in vivo* activity within the intact head. We have approached this goal by constructing a finite element electromagnetic model of a human head and simulating the effect of MREIT protocols with different levels and locations of conductivity changes.

Materials and Methods

We created a three-dimensional finite element model based on a reference MRI data set consisting of 42 sagittal plane slices (3 mm thickness, 270 mm × 270 mm FOV, 512 × 512 matrix size). The model had the same external shape as an adult head, and contained electrically significant structures such as the scalp, skull, subarachnoid space, brain and lateral ventricles. We included spherical anomalies of various diameters inside the brain compartment of the model. The conductivity of these anomalies was chosen to be either the same as the surrounding material (brain) or to have conductivities 1, 3, or 5% higher. Each model was meshed into a large number (ca. 500000) of cubic tetrahedral finite elements (Figure 1b). In our three-anomaly model, 449938 elements were created, with the total number of degrees of freedom around 4.2×10^6. The minimum element quality in the model was about 7×10^{-3}.

Voltage solutions were computed on the head domain, and then converted to B_z values within voxels of size $1.56 \times 1.56 \times 6.8$ mm^3 using the Biot-Savart law. The MR field of view was 200×200 mm^2 and 8 slices were included, each with thickness 6.8 mm. In-slice image matrix size was 128×128. Wires (length 2 cm, conductivity 20000 S/m) were connected to the center of each electrode, and at right angles to each electrode's surface to make the measurement more realistic. Noise was added to the simulated B_z voxel data, based on experimental measurements of B_z noise in the 3T MRI system. We used the single-step harmonic B_z algorithm implemented in CoReHA (conductivity reconstructor using harmonic algorithms) for multi-slice conductivity image reconstructions.

Results and Discussion

Example data from the calculations with and without an anomaly are shown in Figure 2 for the case of 6.4 mA horizontal (LR) current and current application time T_c of 30 ms. The top panel show (a) voltage (in V), (b) current density (in A/m^2) and (c) B_z (in T). The panels below show changes in voltage, current density and B_z when a 5% conductivity increase was introduced into the three anomalies. Changes in B_z due to activity in this case were of the order of $\pm 10^{-11}$ T.

Figure 3 shows reconstructed conductivity images in the case of added noise. Fig 3 (a) and (b) show the original model and local reconstruction area, and a reconstructed noiseless image, respectively. Fig (c) and (d) show reconstructions from B_z data gathered with 8, 16 and 32 averages with and without denoising technique. The 7 and 5 mm anomalies were not clearly visible in images. However, the 10 mm anomaly was consistently apparent in reconstructions. Signal to noise ratios in this case were (without denoising) 11000, 15000 and 21000 for NEX=8, 16 and 32, respectively, and 18000, 20000 and 24000 for corresponding cases with a denoising step added to reconstructions.

Conclusion

We have shown that functional MREIT should be capable of imaging realistically sized conductivity changes occurring within gray matter regions. Future *in vivo* studies will allow us to determine the extent and size of physiological changes.

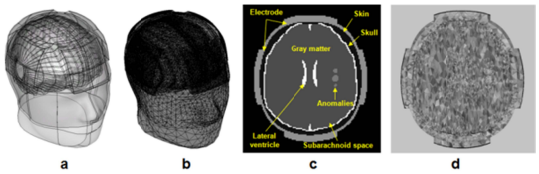

Fig. 1. Overview of complete realistic geometry model. Shown here are (a) brain mesh and electrode placement; (b) completed mesh; (c) cross section of segmented structure; and (d) cross section of mesh.

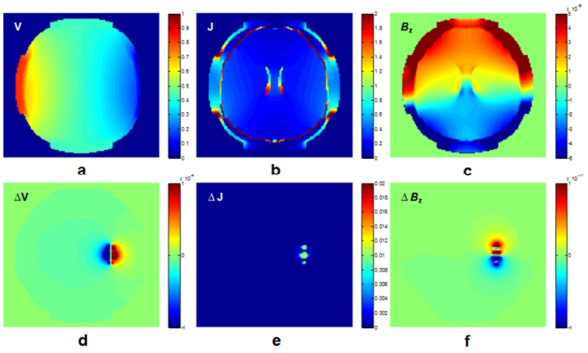

Fig. 2. Central slice showing (a) voltage V, (b) current density magnitude J, and (c) B_z values without anomaly present; and changes caused in the same slice with the 10 mm, 7 mm and 5 mm anomalies having 5% conductivity contrast from brain background as (d) ΔV, (e) ΔJ and (f) ΔB_z distributions.

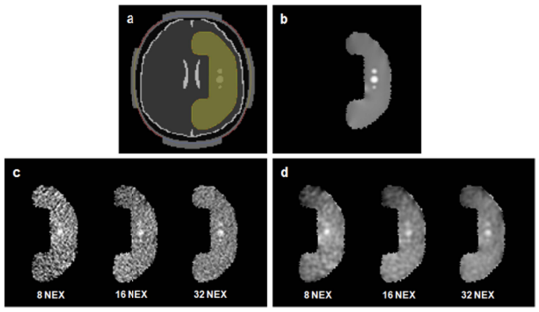

Fig. 3. Locally reconstructed slice of the three-anomaly model with 5% conductivity contrast. (a) original model with reconstruction area highlighted in yellow, (b) reconstruction with no added noise. Images below show reconstructions from B_z data gathered with 8, 16 and 32 averages both with (c) and (d) without denoising technique.

References

1. Tidswell et al, NeuriImage, 13, 283-294, 2001
2. Woo et al, Physiol. Meas., 29, R1-R26, 2008
3. Sadleir et al, NeuroImage, 52, 205-216, 2010